Case Studies in Construction Materials 22 (2025) e04269

Contents lists available at ScienceDirect

Case Studies in Construction Materials

journal homepage: www.elsevier.com/locate/cscm

Sustainable mortar with waste glass fine aggregates and pond ash as an alkali-silica reaction suppressor

W.C.V. Fernando [a,*], W. Lokuge [a], H. Wang [a], C. Gunasekara [b], K. Dhasindrakrishna [a]

[a] School of Engineering, Centre for Future Materials, University of Southern Queensland, Springfield, QLD 4300, Australia
[b] Civil and Infrastructure Engineering, School of Engineering, RMIT University, 124, La Trobe Street, Melbourne, Victoria 3000, Australia

ARTICLE INFO

Keywords:
Recycled glass
Fine aggregate
Pond ash
Supplementary cementitious material
Alkali-Silica Reaction

ABSTRACT

The construction industry seeks sustainable alternatives to conventional materials, with numerous waste types currently destined for landfills offering potential for repurposing. This study examines the replacement of natural sand with crushed waste glass and using pond ash as a supplementary cementitious material in mortar, with a particular focus on mitigating alkali-silica reaction (ASR) and assessing compressive strength. Fly ash, widely recognised for its ASR suppression capabilities, is becoming less available due to the decline in coal-fired power generation, necessitating the exploration of pond ash as a viable alternative. However, given the prolonged storage of pond ash in repositories, its direct substitution for fly ash necessitates thorough investigation. Hence, microstructural and chemical analyses are conducted to investigate the underlying reaction mechanisms. The strength results show that glass can replace natural sand with minimal impact on compressive strength up to 60 %, beyond which strength decreases by 11 % at 100 % glass. However, the ASR expansion results indicate that using more than 20 % glass could lead to long-term detrimental effects. Nevertheless, pond ash effectively mitigates ASR, keeping expansions below 0.1 % at a 10 % OPC replacement, although it performs slightly less efficiently than fly ash. At 20 % replacement, pond ash performs similarly to fly ash. Pond ash outperforms fly ash in 28-day strength up to a 20 % OPC replacement and shows better strength development. The optimal balance between ASR mitigation and compressive strength is achieved with 20 % pond ash, allowing for higher glass utilisation without increasing the risk of ASR.

1. Introduction

Glass is an essential material in modern society, known for its transparency, durability, and versatility in various applications. However, only one-fifth of the globally generated glass waste is beneficially used, and the remainder ends up in landfills [1,2]. Recycling waste glass is a common approach in addressing this issue, although it faces several challenges. The standard method for recycling glass involves sorting, cleaning, and melting waste glass to produce new glass products, a process that consumes a significant amount of energy and resources. Producing high-quality recycled glass is expensive due to impurities and colour variations, making it challenging to meet quality standards [3]. The energy-intensive remelting process adds to the costs and environmental impact of glass recycling [4]. The global glass recycling rate remains relatively low primarily due to the costs associated with conventional remelting methods. As a result, there is a growing interest in finding alternative uses for waste glass to reduce its negative environmental impact

* Corresponding author.
E-mail address: vimukthi.fernando@unisq.edu.au (W.C.V. Fernando).

https://doi.org/10.1016/j.cscm.2025.e04269
Received 22 November 2024; Received in revised form 2 January 2025; Accepted 16 January 2025
Available online 16 January 2025

[5]. One such method involves using it in composite materials such as concrete, bypassing the need for sorting and melting. Waste glass can be crushed into fine or coarse aggregates for use in concrete [6,7] or ground into fine powder to serve as a cementitious material [8]. This method of reusing waste glass conserves landfill space and reduces the demand for river sand extraction, thereby helping to mitigate the negative impacts on river ecosystems.

However, past research has produced conflicting results on the impact of waste glass on the properties of cementitious composites [3,9]. Rashid et al. [7] reported a 22.9 % reduction in concrete compressive strength with 30 % coarse aggregate replaced by crushed waste glass which was attributed to the higher friability [10] and smooth surfaces in glass [7]. Borhan [11] noted a similar strength performance to conventional concrete, even when 100 % of river sand is replaced with glass fine aggregates (GFA). Few researchers have documented a strength increase when glass is employed as a fine aggregate. For instance, Batayneh et al. [12] noted a 40 % strength increase with just 20 % GFA, while Pereira De Oliveira et al. [13] observed a 20 % strength increase with 25 % GFA. A few more studies have reported an increase in compressive strength up to a certain GFA dosage, but a decrease in compressive strength when the dosage was increased beyond that point [14,15]. For example, Rahim et al. [15] observed a strength increase of 31 % at 10 % GFA, followed by strength reduction with increasing GFA levels. Moreover, some studies have shown a clear reduction of strength when any amount of GFA is utilised. For example, De Castro and De Brito [16] observed a reducing trend with increasing GFA percentage. According to Adaway and Wang [14], the enhanced strength compared to the control group can be attributed to the angular and irregular shape of the glass aggregate, which provides a greater surface area compared to naturally rounded sand particles, leading to increased bonding with the cement paste. However, when the GFA content is higher, the aforementioned factors such as the friability of glass and smooth surfaces can lead to the observed reduction of strength.

Furthermore, researchers have identified a major challenge associated with glass-based cementitious composites, namely the alkali-silica reaction (ASR) [17,18]. The amorphous nature of silica found in glass makes it more susceptible to ASR compared to the crystalline silica present in sand [19]. The amorphous silica in GFA reacts with OH^- and alkali metal ions to form an alkali-silicate gel, which can absorb water and increase in volume, as illustrated in Fig. 1 [18–20]. This expansion leads to the development of cracks that compromise the strength and durability of concrete over time [21]. Consequently, researchers have noted higher ASR expansion when crushed glass is used as an aggregate in cementitious composites [6,22,23]. For example, Abdallah and Fan [22] reported a 325 % increase in ASR expansion at 20 % GFA compared to the control, while Ismail and Al-Hashmi [6] observed a 300 % increase under similar conditions. Nonetheless, previous studies revealed that when the glass aggregate size falls within the fine aggregate range (<4.75 mm), the effects of ASR are reduced, especially when the aggregate size is less than 1 mm. Glass particles smaller than 1 mm can exhibit pozzolanic behaviour, reacting with portlandite to form C-S-H gel instead of ASR gel [24,25]. The formation of C-S-H gel also reduces porosity, thereby decreasing permeability and limiting the mobility of ions towards reactive aggregates. Additionally, the C-S-H gel enhances strength, which improves resistance against expansive stresses caused by ASR [24]. The contrasting behaviour in mechanical properties and the potential for ASR expansion could be a key reason why crushed glass is not widely incorporated into concrete in the industry. Hence, researchers have been exploring methods to understand and mitigate ASR, with past studies indicating that replacing ordinary Portland cement (OPC) with low-alkaline supplementary cementitious materials (SCM) such as fly ash (FA) can help reduce ASR occurrence when crushed glass is used as fine aggregates. As an example, Pereira de Oliveira et al. [13] noted a reduction in expansion from 0.014 % to 0.006 % when 30 % of OPC was replaced by FA in concrete containing 50 % GFA.

2. ASR mitigation by pozzolans

Past studies have identified that the addition of pozzolans can mitigate ASR through multiple mechanisms: (i) lowering the alkalinity of the pore solution, (ii) enhancing the microstructure to reduce ionic mobility and water permeability, and (iii) decreasing the availability of calcium (Ca). In blended cement mixes, pozzolans react with $Ca(OH)_2$ to create a denser calcium silicate hydrate (C-S-H) phase that has a lower Ca/Si ratio than the C-S-H produced with the hydration of OPC. These low Ca/Si hydrates are known for

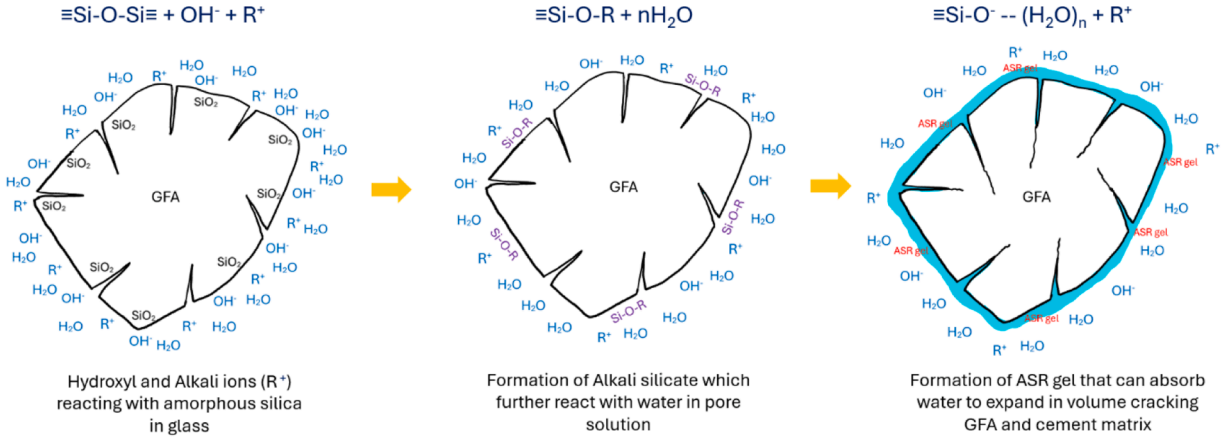

Fig. 1. Simplified ASR reaction for glass mortar.

their alkali retention capabilities, which can dilute the free alkali in the pore solution, thus effectively reducing ASR [26]. Furthermore, Shafaatian et al. [27] observed significantly lower ion diffusivity in FA-based mortar subjected to Accelerated Mortar Bar Test (AMBT) conditions [28], indicating a much slower penetration of NaOH compared to 100 % OPC mortar. The authors attributed this observation to the decreased porosity and capillary pore size in the mortar which is due to the replacement of higher-density OPC with lower-density FA on a mass basis, leading to a net reduction in initial porosity. Hence, this also can contribute to the lower alkalinity of the pore solution, particularly in mortar specimens containing pozzolans that are subjected to AMBT conditions. Moreover, Mugahed Amran et al. [29] observed that the high fineness of FA is improving the microstructure of concrete. The fine FA particles react with the products of the hydration forming a secondary C-S-H gel that fills pores [30]. Several more studies have demonstrated that increasing the amount of FA leads to reduced permeability, sorptivity and chloride penetration properties in cementitious composites which could impede the penetration of NaOH into the AMBT specimens [30,31].

Researchers have noted that the availability of Ca can significantly influence the ASR mechanism in concrete [21]. It has been observed that the reduction of $Ca(OH)_2$ levels, through pozzolanic reactions can mitigate ASR [32]. The presence of $Ca(OH)_2$ is also noted to create semi-permeable reaction rims around reactive sites, which allow alkali metal ions, OH^- and water to penetrate while blocking others, leading to material buildup and expansion [33]. Additionally, $Ca(OH)_2$ helps maintain a high pH in the pore solution and contributes to ion exchange processes that exacerbate the formation of swelling alkali-silica complexes [21].

3. Research significance

While the potential of FA to alleviate ASR in glass concrete has been explored by researchers, further investigations are deemed imperative to ascertain the practical viability of FA and GFA-based cementitious composite applications. Additionally, with the closure of coal power plants, the availability of FA is becoming scarce, necessitating the exploration of alternative materials to replace FA. Nevertheless, another often-overlooked byproduct of the coal industry, pond ash (PA), holds the potential for mitigating ASR in concrete, similar to FA. By-products of coal combustion are primarily categorised into FA, constituting around 70–90 %, and bottom ash (BA), accounting for 10–20 % [34]. Collected FA undergoes processes such as drying, separation, and grinding to produce the commercial SCM with high pozzolanic activity [35]. Pond ash refers to the waste component, comprising a mixture of unprocessed and unutilised FA and BA, and therefore exhibits a lower pozzolanic ability compared to FA [36,37]. Traditionally, PA finds its way to outdoor ash ponds or storage tanks/silos, where it may be susceptible to impurities and moisture contamination. In 2016, global coal combustion ash production was reported as 1221.9 million metric tons (Mt) per year, with only 63.9 % of it being utilised, leaving 544.2 Mt as waste [38]. A report released in 2019 [36] revealed coal ash waste accounts for nearly one-fifth of Australia's industrial waste stream and a survey done in 2022 showed that approximately 5.1 million tonnes of ash waste were placed into onsite storage ponds awaiting some future use opportunity [39]. This disposal method raises concerns regarding potential environmental impacts, especially when stored in ponds, as it directly exposes the waste to the environment [36]. Hence, it becomes imperative to seek methods to reclaim and reuse this resource, thereby minimizing exposure to the environment. However, due to prolonged exposure to environmental conditions and its composition as a mixture of unprocessed FA and BA, further investigations are required to assess the viability of PA as a suitable alternative to commercial FA.

Previous studies have shown that the inclusion of PA reduces the strength of cementitious composites. Yimam et al. [37] and Phanikumar & Sofi [40] reported reductions of 19.2 % and 7.1 %, respectively, in the 28-day compressive strength of concrete containing 30 % PA. Patrisia et al. [41] demonstrated the viability of utilising 15 % pond ash along with 20 % GFA in structural concrete blocks. However, research investigating the use of PA as an ASR mitigating SCM in cementitious mortar is limited, especially in combination with GFA. Hence, this study sets out to investigate the efficacy of incorporating PA as an SCM in mitigating ASR in GFA-mortar. Furthermore, the research aims to draw comparisons between the ASR mitigation capabilities of PA and FA, given that both materials are derived through similar processes and may share characteristics of low alkalinity. Moreover, since the ability to mitigate ASR alone is not sufficient to determine its suitability as an alternative for OPC in mortar, this study also includes an investigation of GFA mortar strength. This comprehensive exploration aims to contribute valuable insights into sustainable practices and environmentally conscious applications within the concrete industry, focusing on cement substitution with PA and sand substitution with GFA to enable the production of lower-impact cementitious composites.

4. Materials and test methods

4.1. Materials

This study utilised OPC as the primary cementitious material, and commercially available river sand as the primary fine aggregate.

Table 1
Physical properties of GFA and river sand.

Property	Sand	GFA
Moisture content (%)	3.9	1
Water absorption (%)	0.48	0.3
Dry density (kg/m3)	2627	2438
SSD density (kg/m3)	2640	2451

Crushed waste glass with a maximum aggregate size of 4.75 mm, procured from IQrenew based in Queensland, Australia, was incorporated as a sustainable substitute for river sand in mortar. This crushed waste glass is not colour-sorted and hence contains various types of glass. To tackle the potential ASR that could arise due to the use of GFA, the study employed PA as an SCM, strategically substituting for OPC. The widely accepted FA (Class-F) as an ASR mitigation SCM was used as a comparison for PA. The PA utilised in this research was sourced from one of the power stations in Queensland, Australia and sieved to ensure a particle size smaller than 45 μm, thereby enhancing its reactivity. A commercially available class-F FA product was utilised in this study.

Table 1 presents the physical properties of both GFA and river sand. The moisture content was measured following the standardized procedure outlined in ASTM C566 [42]. Furthermore, the absorption and densities of the materials were assessed following the guidelines given in ASTM C128 [43]. River sand exhibited a significantly higher moisture content and moisture absorption in comparison to glass. The water absorption characteristics of river sand can be attributed to the porous nature of its grain surfaces as evidenced by the scanning electron microscopy (SEM) images presented in Fig. 2(a). The water absorption exhibited by GFA can be explained by the presence of microscopic cracks within its grains as shown in Fig. 2(b). Moreover, as outlined in Table 1, the density of glass is 7 % lower than that of river sand.

Fig. 3(a) offers a visual comparison of the grading between GFA and river sand, providing a detailed illustration in accordance with the specifications outlined by ASTM C33 [44]. Both the utilised river sand and GFA fall well within the specified range defined by ASTM C33 for fine aggregates. This confirms the suitability of GFA as a replacement for river sand.

Fig. 3(b) displays the average particle sizes of the cementitious materials employed, as measured by analysing dry samples of each material with a laser particle size analyser. The data shows that PA has larger particles compared to both OPC and FA. The chemical compositions of OPC, FA, and PA were analysed using X-ray fluorescence (XRF) and the findings are detailed in Table 2. The results indicate that PA has a lower CaO content compared to OPC, which is consistent with its origin as a coal combustion product, similar to class-F FA. According to ASTM C618 [45], the PA used in this study can be classified as a Class-F pozzolan, since the total $SiO_2 + Al_2O_3 + Fe_2O_3$ content exceeds 70 %, and the CaO content is less than 18 %. This suggests a plausible expectation that PA may also contribute to the mitigation of ASR. It is also noted that PA has marginally higher alumina and silica compared to FA.

4.2. Mix design and specimen preparation

The mix proportions were chosen to assess the ASR expansion and strength of mortar incorporating GFA, FA, and PA, as shown in Table 3. River sand was substituted with GFA in 20 % increments, ranging from 0 % to 100 %, to investigate the influence of replacement levels on the targeted properties. Furthermore, the same set of mixes was repeated with PA and FA replacing 10 %, 20 %, and 30 % of OPC. In all mixes, the water content and water/binder ratio were kept constant at 205 kg/m^3 and 0.44, respectively. This particular variation allows the examination of the impact of PA on the mortar while providing a comparison with FA. In all mixes, the total cement and fine aggregate contents were 466 kg/m^3 and 581 kg/m^3, respectively. Additionally, relying on the aforementioned moisture content and water absorption data of aggregates, the mixes were appropriately adjusted with varying GFA percentages to maintain consistent water content across all mixes. This adjustment ensures a more equitable comparison between the mixes, as fluctuating water content can impact both strength and workability. The mortar mixing process was performed utilising a benchtop mixer. Moreover, admixtures were not used to modify the mixes, as the purpose of this study is to investigate the direct effect of including GFA and PA on the mortar.

4.3. Flow test

The flow of all mixes was measured according to the standards set by the ASTM C1437 specifications [46] as it is a good indicator for the workability of mortar. This evaluation was carried out using a flow table designed for tests of hydraulic cement.

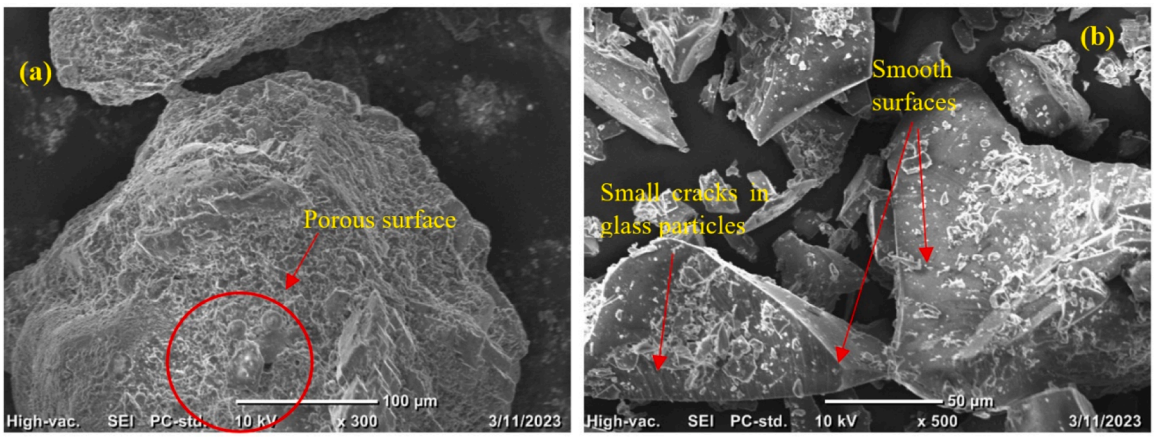

Fig. 2. SEM images of; (a) the porous nature of river sand grains; (b) microscopic cracks in GFA.

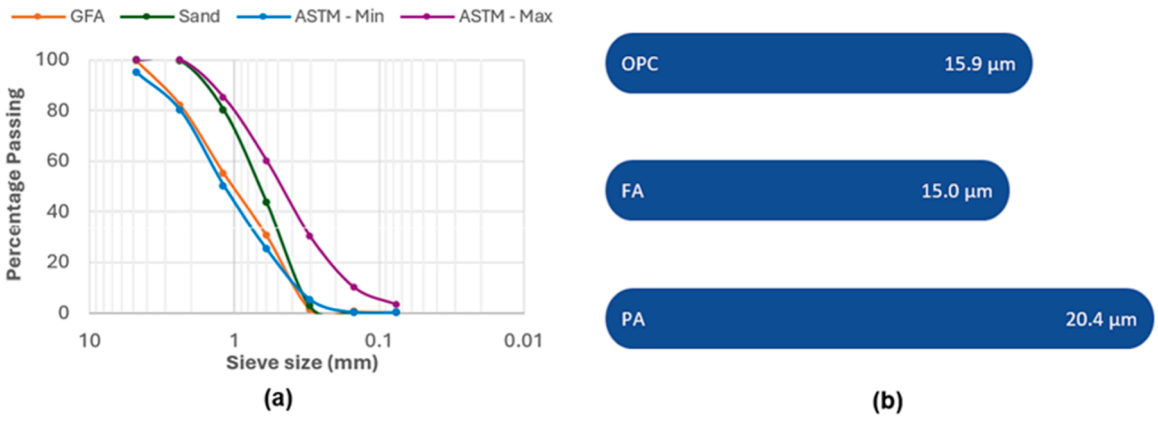

Fig. 3. (a) Particle size distributions of sand and GFA; (b) mean particle sizes of OPC, FA and PA.

4.4. Accelerated mortar bar test (ASTM C1567)

The Accelerated Mortar Bar Test (AMBT) was conducted in accordance with ASTM C1567 [28] to investigate the impact of replacing river sand with GFA and replacing OPC with PA on ASR expansion. FA is used as a comparison for PA. Three mortar specimens were prepared for each mix, with dimensions of 25 × 25 x 280 mm. The standard procedure encompassed curing the specimens for 24 hours in the moulds, immersing them in a water bath for an additional 24 hours at 80°C after demoulding, and subsequently placing them in a sealed container with a 1 M NaOH solution at 80°C. Over the ensuing 14 days, the changes in the length of the mortar bars were monitored by taking at least 3 intermediate readings. The monitoring involved drying the surface of the bars, followed by precise length measurements utilising a vertical comparator with a precision of less than 0.002 mm. According to ASTM C1567, combinations of Portland cement, SCMs, and aggregates are classified as potentially innocuous if the ASR expansion at 14 days is below 0.1 %, and as reactive and deleterious if it exceeds 0.2 %. ASR expansion between 0.1 % and 0.2 % indicates potential deleterious behaviour with slow reactivity. Hence, it is crucial to reduce the ASR expansion to below 0.1 % to achieve effective ASR mitigation.

4.5. Thermogravimetric analysis

Thermogravimetric Analysis (TGA) was conducted on 28-day paste samples containing 100 % OPC, 20 % FA, and 20 % PA to investigate how the low CaO content of PA and FA affect cement hydration by measuring the residual $Ca(OH)_2$. The 100 % OPC specimen served as the control for comparison when a fixed amount of OPC was replaced with PA and FA. The 20 % replacement level was selected as the reference value, representing the intermediate level among the replacement percentages considered in this study: 10 %, 20 %, and 30 %. The TGA test was performed over a temperature range of 30–1000°C at a scanning rate of 20 °C/min using the TGA Q500 instrument in a nitrogen environment. Specifically, the analysis aimed to investigate the dehydroxylation process, which involves the decomposition of $Ca(OH)_2$. The thermogravimetric curves were examined using the tangential method, which involves determining the temperature range of dehydroxylation from the derivative of the weight versus temperature graph shown in Fig. 4(b). After identifying this temperature range, the weight loss associated with dehydroxylation is calculated using the weight versus temperature graph shown in Fig. 4(a). From this weight loss, the quantity of $Ca(OH)_2$ that is present in the samples can be calculated, offering information on the hydration behaviour influenced by the incorporation of both SCMs.

4.6. Pore solution extraction and analysis

A pore solution analysis of AMBT specimens was conducted by assessing the pH value and Na^+ content in the extracted pore solutions. The pore solution extraction was done using the cold-water extraction method [23]. The middle section of AMBT specimens, approximately 2 in. in length, was extracted at 14 days and crushed using a hammer, followed by further grinding with a mortar and pestle to produce a fine powder. To extract the pore solution, a suspension was prepared by combining 2.5 g of powdered solid samples with 50 g of deionized water. The mixture was stirred on a magnet stirrer at 800 rpm for 5 minutes to facilitate the leaching of ions from the pore solution. The mixture was subsequently filtered, and the pH of the resulting solution was measured using a pH meter. Subsequently, the Na^+ ion content in the extracted solution was determined using an Atomic Absorption Spectrophotometer (AAS).

4.7. SEM imaging

A microscopic investigation was conducted through the acquisition of SEM images of various mortar specimens. The SEM imaging process focused on samples extracted from specific 91-day compressive strength specimens and AMBT specimens. The choice to examine the 91-day specimens instead of the 28-day specimens was deliberate, aiming to explore the potential presence of ASR gel

Table 2
Chemical compositions of the OPC, FA and PA.

Material	Composition (%)														
	Al2O3	BaO	CaO	Cr_2O_3	Fe_2O_3	K_2O	MgO	MnO	Na_2O	P_2O_5	SO_3	SiO_2	SrO	TiO_2	LOI
OPC	4.27	0.03	> 60	0.02	3.39	0.61	3.35	0.24	0.12	0.14	2.86	19.5	0.07	0.23	2.85
FA	25.02	0.1	4.56	0.01	6.9	0.88	1.29	0.09	0.3	0.61	0.25	56.28	0.05	1.34	2.17
PA	31.15	0.09	1.58	< 0.01	3.04	0.52	1.3	0.04	0.54	0.05	0.07	59.29	0.04	1.64	0.27

Table 3
Mix ratios.

Mix designations		MIX PROPORTIONS									
		Cement/Binder (kg/m^3)					water content (kg/m^3)	water/binder ratio	Fine aggregate (kg/m^3)		
		OPC	Fly ash	Fly ash %	Pond ash	Pond ash %			Sand	GFA	GFA %
0FA - 0PA	0GFA	466	-	-	-	-	205	0.44	581	0	0
	20GFA	466	-	-	-	-	205	0.44	465	116	20
	40GFA	466	-	-	-	-	205	0.44	349	232	40
	60GFA	466	-	-	-	-	205	0.44	232	349	60
	80GFA	466	-	-	-	-	205	0.44	116	465	80
	100GFA	466	-	-	-	-	205	0.44	0	581	100
10FA - 0PA	0GFA	419	47	10	-	-	205	0.44	581	0	0
	20GFA	419	47	10	-	-	205	0.44	465	116	20
	40GFA	419	47	10	-	-	205	0.44	349	232	40
	60GFA	419	47	10	-	-	205	0.44	232	349	60
	80GFA	419	47	10	-	-	205	0.44	116	465	80
	100GFA	419	47	10	-	-	205	0.44	0	581	100
20FA - 0PA	0GFA	373	93	20	-	-	205	0.44	581	0	0
	20GFA	373	93	20	-	-	205	0.44	465	116	20
	40GFA	373	93	20	-	-	205	0.44	349	232	40
	60GFA	373	93	20	-	-	205	0.44	232	349	60
	80GFA	373	93	20	-	-	205	0.44	116	465	80
	100GFA	373	93	20	-	-	205	0.44	0	581	100
30FA - 0PA	0GFA	326	140	30	-	-	205	0.44	581	0	0
	20GFA	326	140	30	-	-	205	0.44	465	116	20
	40GFA	326	140	30	-	-	205	0.44	349	232	40
	60GFA	326	140	30	-	-	205	0.44	232	349	60
	80GFA	326	140	30	-	-	205	0.44	116	465	80
	100GFA	326	140	30	-	-	205	0.44	0	581	100
0FA - 10PA	0GFA	419	-	-	47	10	205	0.44	581	0	0
	20GFA	419	-	-	47	10	205	0.44	465	116	20
	40GFA	419	-	-	47	10	205	0.44	349	232	40
	60GFA	419	-	-	47	10	205	0.44	232	349	60
	80GFA	419	-	-	47	10	205	0.44	116	465	80
	100GFA	419	-	-	47	10	205	0.44	0	581	100
0FA - 20PA	0GFA	373	-	-	93	20	205	0.44	581	0	0
	20GFA	373	-	-	93	20	205	0.44	465	116	20
	40GFA	373	-	-	93	20	205	0.44	349	232	40
	60GFA	373	-	-	93	20	205	0.44	232	349	60
	80GFA	373	-	-	93	20	205	0.44	116	465	80
	100GFA	373	-	-	93	20	205	0.44	0	581	100
0FA - 30PA	0GFA	326	-	-	140	30	205	0.44	581	0	0
	20GFA	326	-	-	140	30	205	0.44	465	116	20
	40GFA	326	-	-	140	30	205	0.44	349	232	40
	60GFA	326	-	-	140	30	205	0.44	232	349	60
	80GFA	326	-	-	140	30	205	0.44	116	465	80
	100GFA	326	-	-	140	30	205	0.44	0	581	100

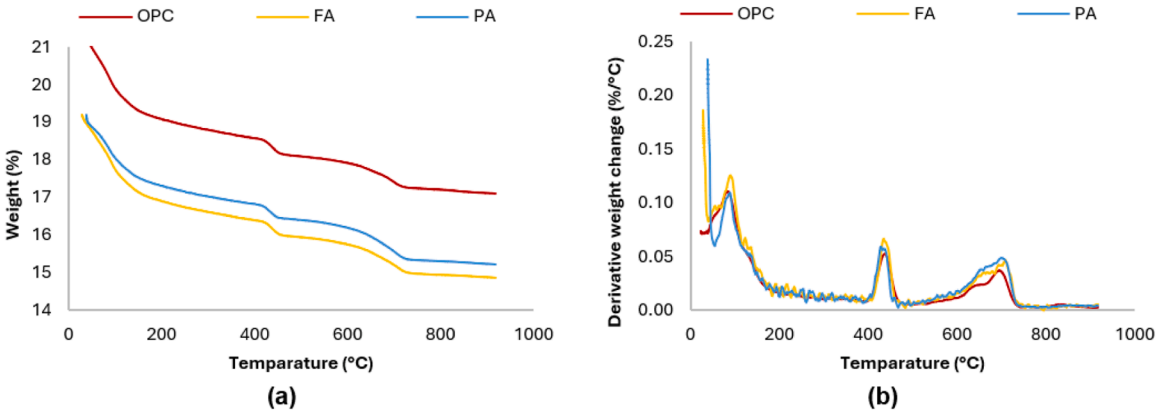

Fig. 4. TGA results; (a) Weight vs temperature; (b) Weight derivative vs temperature.

since ASR is a phenomenon that develops over an extended period rather than a short term, hence the rationale behind this selection. The extracted samples were immediately sealed in plastic bags until the SEM imaging to avoid carbonation; however, some extent of carbonation was unavoidable.

4.8. Compressive strength test

The compressive strength tests were conducted on mortar specimens with dimensions of 40 × 40 x 40 mm, following the protocols outlined in ASTM C109 [47]. The strength measurements were taken at 28 days and additionally at 91 days using a concrete tester. The 91-day compressive strength testing was conducted to assess the long-term strength development ability of used SCMs and to investigate if there are any potential deleterious effects arising from ASR. To ensure precise load measurements, a load cell with a capacity of 300 kN was employed in conjunction with the compressive strength test machine. For each mix 6 mortar cubes were cast and cured in a curing room with 100 % relative humidity before testing at 28 and 91 days.

5. Results and discussion

5.1. ASR behaviour with increasing GFA in OPC mortar

This research further confirms the past findings for OPC-based GFA-mortar, as an increase in ASR expansion was observed with the increasing percentage of GFA, as demonstrated in Fig. 5. When the GFA percentage exceeds 20 %, the ASR expansion falls within the range of 0.1 % and 0.2 %, indicating a potential for deleterious effects from ASR. The 20 % GFA mix exhibits ASR expansions slightly below 0.1 %; however, it may still display long-term effects of ASR. This highlights that incorporating GFA in mortar can lead to potentially harmful effects unless ASR mitigation techniques are employed. Therefore, this study investigates the use of PA for ASR mitigation, with FA included for comparative analysis, and the findings are presented in Fig. 5.

5.2. Effect of fly ash and pond ash as an ASR mitigation technique

The partial substitution of PA for OPC significantly reduces ASR expansion, which is observed even in mixes without GFA, as shown in Fig. 5. All mixes with varying percentages of PA exhibit ASR expansions below the 0.1 % threshold, suggesting their potentially innocuous nature. For the 10 % PA mix, the ASR expansion remains slightly below 0.1 % across all GFA levels, still significantly lower than the ASR expansion observed in 100 % OPC mixes. However, despite PA containing less CaO than FA as shown in Table 2, which theoretically should enhance ASR mitigation, its performance is lower. For instance, at 100 % GFA, the mix containing 10 % FA exhibited a 0.04 % ASR expansion, while the 100 % GFA mix with 10 % PA showed a higher value of 0.08 %, just below the 0.1 % threshold. At a 20 % OPC replacement level, FA slightly outperforms PA, except at 100 % GFA content, where PA and FA exhibit similar performance. This suggests that PA can be a viable alternative to FA for ASR mitigation, particularly at the 20 % OPC replacement level.

Furthermore, as shown in Fig. 5, another trend emerges with the increasing percentage of GFA in PA and FA mixtures, where a reduction in ASR expansion is observed. This contrasts with the observations in AMBT specimens containing only OPC. The same phenomenon can be observed with FA as well. This phenomenon can be attributed to GFA aggregates within the mortar acting as a barrier that impedes the seepage of NaOH solution into the specimen, facilitated by the impermeable nature of glass. This effect is discussed in past studies explaining the diminished permeability, sorptivity and chloride penetration when crushed glass is used as an aggregate in cementitious composites [13,48]. This effect is not observed in OPC mixes, as it is overshadowed by the ASR expansion. However, in the presence of PA and FA, the ASR expansion is mitigated, allowing this effect to become noticeable.

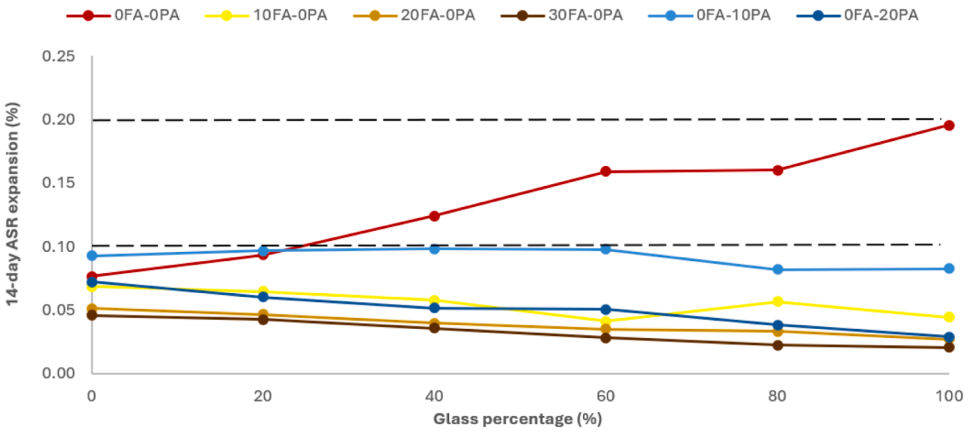

Fig. 5. 14-day ASR expansion for varying GFA, FA and PA percentages in AMBT.

These observations can be further explained using the TGA results, which determine the availability of $Ca(OH)_2$, microscopic behaviour by SEM imaging and, pore solution analysis.

5.2.1. Ca availability

By substituting high-calcium OPC with low-calcium PA, the available CaO content for cement hydration is reduced. This, in turn, decreases portlandite ($Ca(OH)_2$) formation, which contributes to the observed reduction of ASR, as discussed in Section 2. This dilution effect is evident in the TGA results shown in Fig. 6, where 20 % of OPC was replaced with PA in cementitious paste specimens. These results indicate that replacing 20 % of OPC has reduced the $Ca(OH)_2$ content in the paste specimen by approximately 20 %. The same effect can be observed for FA in the same figure, attributed to its similarly low calcium content. Moreover, due to the slightly lower amount of CaO in PA compared to FA, a slight reduction of $Ca(OH)_2$ can be observed with PA. However, this reduction is not as pronounced in ASR expansion results, as FA performs better than PA in ASR mitigation. The lower $Ca(OH)_2$ content in the PA specimen should make it more effective than FA for ASR mitigation. This discrepancy can be explained through microscopic observations.

5.2.2. Microscopic observation

Fig. 7 presents SEM images of AMBT specimens, both without GFA (Figures (a), (b) and (c)) and with 100 % GFA (Figures (d), (e) and (f)), for different mix compositions: 100 % OPC, 20 % FA, and 20 % PA. Compared to the 100 % OPC mix without GFA (Fig. 7(a)), the SEM image of the 100 % GFA mix in Fig. 7(d) shows a white substance on the surface of the glass aggregate, likely ASR gel, consistent with findings from previous studies [49–51]. This white substance is not visible in the mix without GFA, as shown in Fig. 7 (a). This observation further supports the increase in ASR expansion with higher GFA content.

The SEM images of AMBT specimens with 100 % GFA and 20 % PA in Fig. 7(f) reveal the absence of ASR gel compared to the mix with 100 % GFA and OPC as shown in Fig. 7(d). Similar behaviour can be observed in the FA mix due to its ASR mitigation ability. This absence of ASR gel in the PA mix further supports the effectiveness of PA in reducing ASR expansion.

A comparison of Figs. 7(b) and 2(c) reveals that the PA mortar displays a less favourable microstructure than FA, characterized by the presence of microcracks that potentially reduce the impedance against external NaOH penetration. This weaker microstructure in PA specimens likely contributes to the observed lower ASR mitigation ability of PA. Past studies have attributed this improved microstructure in FA to the pozzolanic reaction of FA and the increased volume of FA resulting from the replacement of OPC on a mass basis. Even though a similar improved microstructure might be expected from PA due to its similar pozzolanic composition to FA and the lower density compared to OPC, the observations indicate otherwise. The smaller particle size of FA, which increases reactivity, could play a role in improving the microstructure compared to PA. Moreover, Najafi Kani et al. [52] reported that the addition of 3 % nano-Fe_2O_3 resulted in a densified microstructure in cementitious composites due to insoluble Fe_2O_3 filling the voids of the C-S-H gel structure. This could have also contributed to the better microstructure of FA compared to PA, as FA contains 6.9 % Fe_2O_3, whereas PA contains only 3.04 % Fe_2O_3. The difference in Fe_2O_3 content and the resulting improved microstructure explain the better ASR mitigation ability of FA than PA, even though PA contains less CaO, which should theoretically improve its ASR mitigation ability. However, the form of Fe_2O_3 in SCMs may not be at the nanoscale, but due to its insoluble nature, it can be assumed that similar to nano-Fe_2O_3, the Fe_2O_3 in SCMs can also fill the voids. Additionally, the ASR expansion test could not be conducted for the 30 % PA mix due to its lower strength, resulting in breakage during demolding. This issue likely stemmed from the weaker microstructure observed in PA specimens.

5.2.3. Pore solution analysis

The pH value of the pore solution analysis, presented in Fig. 8, shows a slight increase when GFA content has increased to 100 % in OPC-only mixes. This increase can be attributed to the increasing ASR expansion, allowing more OH^- ions to seep into the specimen. However, the Na^+ concentration of the pore solution analysis, depicted in Fig. 8, shows a steep reduction. This reduction indicates that the seeped Na^+ ions are retained within the formed ASR gel, preventing them from being extracted during the pore solution extraction process.

The higher levels of OH^- and Na^+ in PA specimens compared to FA reflect their weaker microstructure, which offers less resistance to ion penetration from NaOH solution. Nevertheless, both the 0 % and 100 % GFA-PA mixes still exhibited lower ion penetration compared to OPC specimens, indicating that PA still provides better ion resistance than 100 % OPC specimens and thereby better ASR performance compared to OPC. In contrast, the enhanced microstructure of FA specimens, which can impede NaOH penetration, is corroborated by pore solution analysis. FA specimens with both 0 % and 100 % GFA displayed lower pH values and Na^+

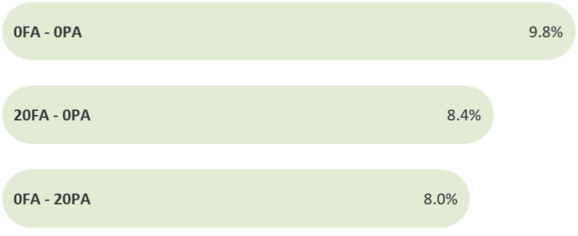

Fig. 6. $Ca(OH)_2$ percentage of paste samples from TGA results.

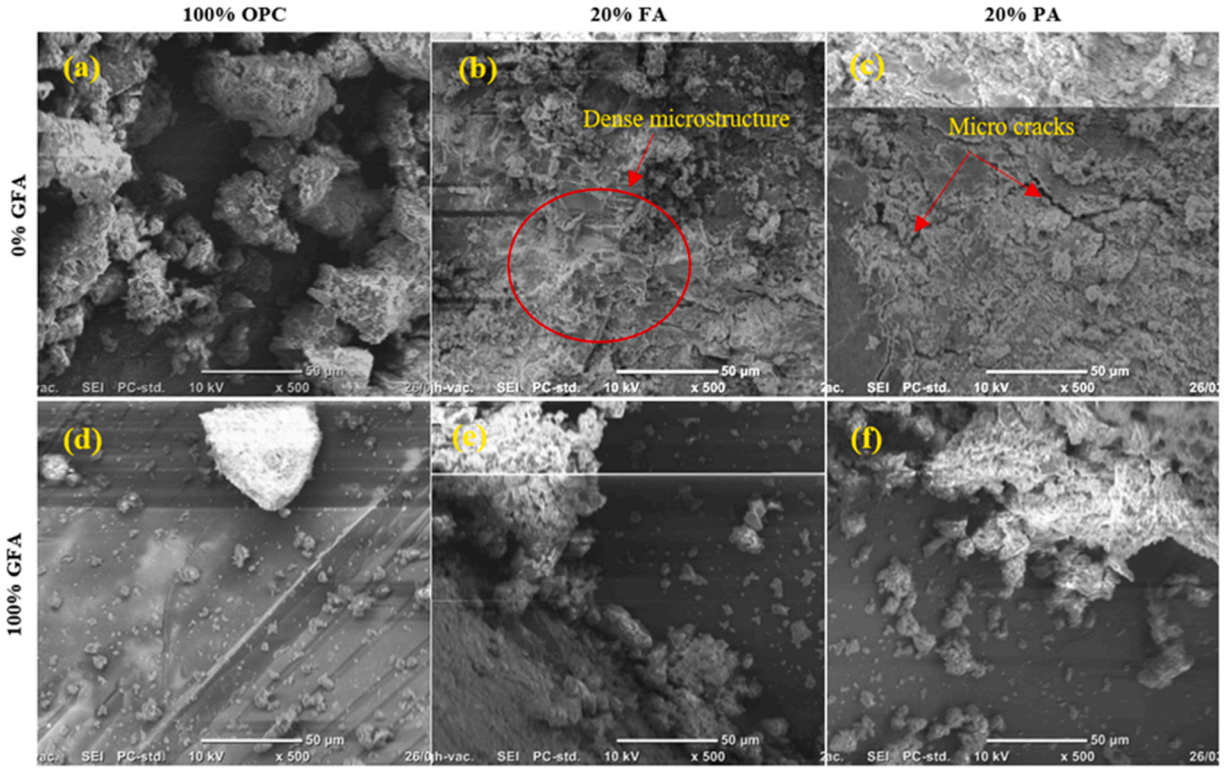

Fig. 7. SEM images showing the microstructure of AMBT specimens; (a) 0 % GFA and 100 % OPC; (b) 0 % GFA and 20 % FA; (c) 0 % GFA and 20 % PA; (d) 100 % GFA and 100 % OPC; (e) 100 % GFA and 20 % FA; (f) 100 % GFA and 20 % PA.

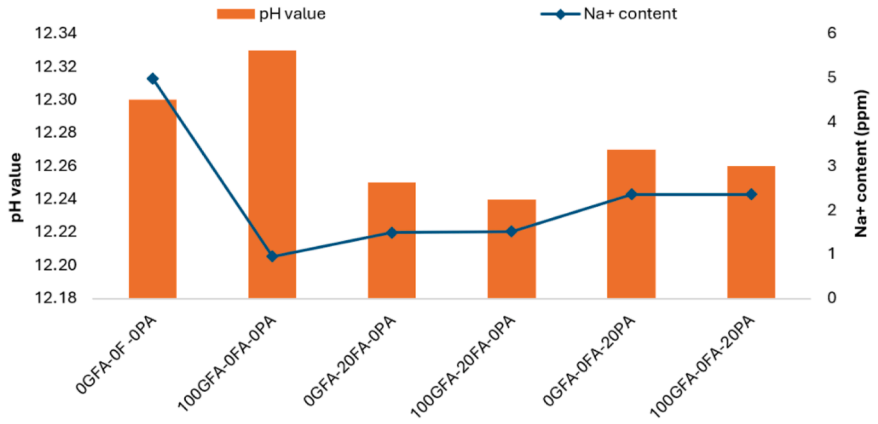

Fig. 8. pH value and Na^+ content in pore solutions.

concentrations compared to all other mixes except the 100 % GFA and OPC mix, suggesting a reduced ability for OH^- and Na^+ ions to infiltrate these samples. In addition to the improved microstructure, the formation of low Ca/Si hydrates due to the pozzolanic reaction of both PA and FA can also retain alkalis, as indicated by past studies. This retention of alkalis could contribute to the reduced OH^- and Na^+ content observed in both PA and FA mixes compared to the 0 % GFA and 100 % OPC mix.

Fig. 8 reveals that both PA and FA mixes show a slight decrease in pH values as the percentage of GFA increases from 0 % to 100 %, which contrasts with the behaviour observed in 100 % OPC mixes. As PA and FA suppress ASR expansion, OH^- ions cannot penetrate the specimens in the same manner as with the 100 % GFA OPC-only mix. This allows the impermeable barrier effect of GFA to take effect. As the GFA content increases, the less potential for OH^- penetration due to the impermeable glass barriers. The Na^+ content exhibits a slight increase, as suppressed ASR results in fewer ASR products available to retain Na^+. This observation aligns with the previous observation discussed above, where, in OPC-only 100 % GFA specimens, the Na^+ content demonstrated a notable decrease when abundant ASR products were available to retain Na^+.

5.3. Effect of GFA on the strength of OPC mortar

Fig. 9 demonstrates the trend for the 28-day and 91-day compressive strength of OPC mortar with increasing content of GFA. Until 60 % GFA, the 28-day mortar strength exhibits very similar performance to conventional mortar, after which it shows a decreasing trend, reporting a strength reduction of 11 % at 100 % GFA. Fig. 9 reaffirms this behaviour also in 91-day strength, suggesting that GFA can effectively mimic the strength performance of river sand. The reduction in strength at higher levels of GFA can be attributed to various factors. The increased friability of glass compared to sand, along with the crushing process of waste glass, can lead to residual cracks in GFA grains [53] as evidenced by Figs. 2(b) and 12. These residual cracks and the higher friability can increase the tendency of GFA to crack under stress, which contributes to a reduction in the overall strength of the material. The smoother surfaces of glass aggregates compared to sand can lead to a weaker bond between GFA and the cement matrix, thereby reducing the strength. Damrongwiriyanupap et al. [54] and Ling and Poon [55] discussed this effect of strength reduction due to the weaker bond at the interfacial transition zone of GFA in mortar. This smoother texture also increases workability due to the reduced friction between aggregates [51], as evidenced by the flow results presented in Fig. 10. The increased workability can elevate the tendency for the segregation of GFA, further contributing to the observed reduction in strength.

5.4. Effect of the addition of pond ash and fly ash on strength

Fig. 9 further presents the 28 and 91-day strength results for different percentages of PA while comparing the same with its counterparts of OPC and FA mixes. In both 28 and 91-day results, a general trend of strength reduction is observed for both PA and FA compared to the 100 % OPC mixes in all OPC replacement percentages. Moreover, a trend of reducing strength can be observed with the increasing percentages of both SCMs. This is caused by the dilution effect of quicklime (CaO), in total cement content since OPC is replaced by SCMs with low CaO content (Table 1). As discussed before, the TGA results show a decrease in the presence of residual Ca$(OH)_2$ when 20 % of OPC is substituted with either PA or FA in paste specimens at 28 days. Ca$(OH)_2$ is a byproduct of the hydration of CaO, a crucial reaction contributing to strength. Therefore, the significantly diminished levels of Ca$(OH)_2$ indicate reduced hydration of cement when both SCMs are utilised as replacements for OPC. However, the pozzolanic reactions of PA or FA can also consume Ca$(OH)_2$ causing the observed reduction on top of the dilution effect. Nevertheless, the reduction percentage of Ca$(OH)_2$ only reflects the

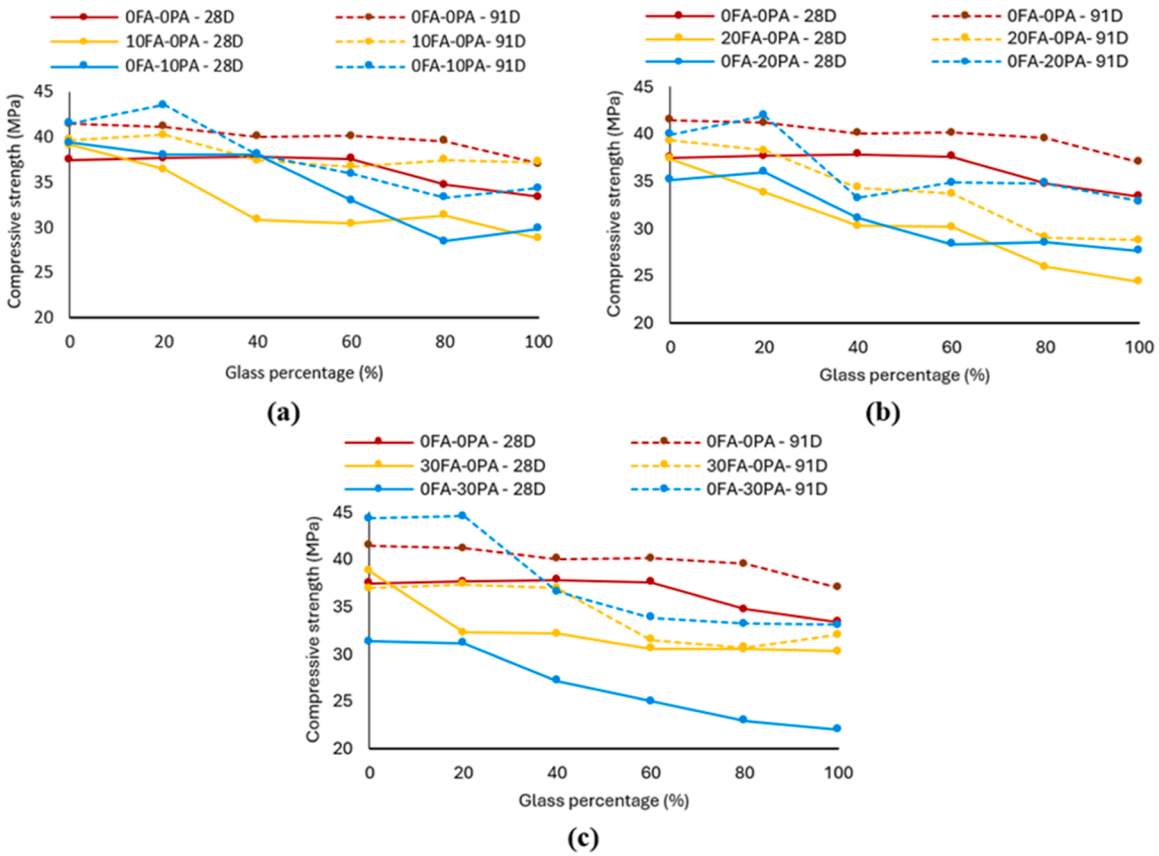

Fig. 9. Compressive strength results; (a) 28 and 91-days strength of control, 10 % FA and 10 % PA; (b) 28 and 91-days strength of control, 20 % FA and 20 % PA; (c) 28 and 91-days strength of control, 30 % FA and 30 % PA.

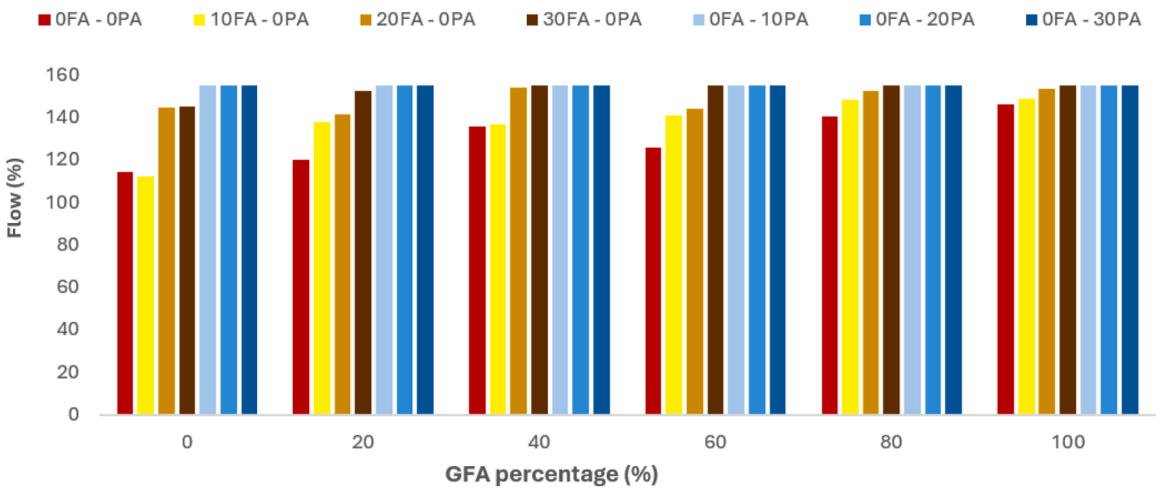

Fig. 10. Flow values of GFA mortar with varying percentages of GFA, FA and PA.

dilution effect since the reduction of $Ca(OH)_2$ for both 20 % PA and FA mixes is approximately 20 % in TGA results indicating the negligible pozzolanic reactivity of both SCMs at 28 days. This suggests that replacing OPC with PA and FA has contributed to the observed reduction of 28-day mortar strength mainly due to the dilution effect.

The inclusion of PA and FA has notably enhanced the workability of GFA mortar, as indicated by the flow results in Fig. 10. This improvement in the flow can be attributed to the spherical shape and smoother surface of PA and FA particles, shown in Fig. 11. These characteristics help to reduce inter-particle friction through a ball-bearing effect, thereby enhancing the flowability of the cement mixture compared to the irregular shapes of OPC particles [56–58]. According to Moghaddam et al. [56], the low water absorption capacity of fly ash particles, attributed to their inherent glassy and smooth texture compared to OPC particles, could also explain the improved flowability. This reasoning can similarly be applied to PA particles, which exhibit a comparable texture. Therefore, just as increasing GFA content increases workability and the tendency for aggregate segregation, which can lead to strength reduction, the addition of both SCMs may similarly impact strength.

It can be observed that, compared to FA, PA exhibits a more significant reduction in 28-day strength as the OPC replacement percentage increases. In Fig. 9(a), it is observed that 10 % of PA performs better than FA until 60 % of GFA while performing similarly to the control until 40 % of GFA. After 60 % GFA, both SCMs perform similarly with slight fluctuations. At 20 % OPC replacement, both PA and FA perform similarly, while showing significantly lower strengths than 100 % OPC mixes, as shown in Fig. 9(b). However, PA performed slightly better than FA after 80 % GFA. Fig. 9(c) shows that when the PA percentage is increased to 30 %, it significantly underperforms compared to both FA and OPC beyond 20 % GFA.

The reduction in strength with the increasing percentage of PA compared to FA can be attributed to several factors. As evidenced by Fig. 10, PA mixes demonstrate significantly higher workability compared to FA since even 10 % of PA shows higher flow than 30 % of FA. This difference may be attributed to the more clustered nature of FA particles, as shown in Fig. 11(b). In contrast, the particles in PA appear to be less clustered (Fig. 11(c)), which can result in reduced inter-particle friction compared to FA. This reduced friction can lead to the observed higher flowability of PA, increasing the tendency for segregation and contributing to the observed reduction in strength. Moreover, PA consists of larger particles compared to FA, as also evidenced by Fig. 11(c), which could reduce the reactivity of PA and contribute to its lower observed strength. Furthermore, the TGA results discussed in Section 5.2.1, showed a slightly lower amount of $Ca(OH)_2$ indicating slightly reduced hydration in the PA paste at 28 days compared to FA, attributed to the higher dilution of CaO since PA contains less CaO than FA, as shown in Table 1. This could also contribute to the observed decrease in strength with PA.

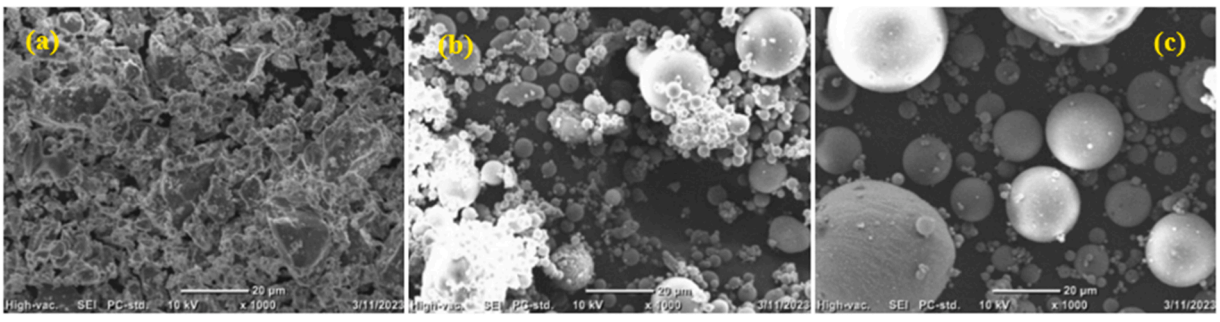

Fig. 11. SEM images of; (a) OPC; (b) FA; (c) PA.

Thus, while both PA and FA lead to strength reductions due to the dilution effect, the higher workability, lower particle reactivity and slightly higher calcium dilution of PA result in a more pronounced reduction in strength compared to FA at 28 days.

Nevertheless, at 91 days, different behaviour can be observed for PA as shown in Fig. 9. In almost all OPC replacement percentages, PA shows better performance than FA, unlike in the 28-day results. Also, a few more trends of PA compared to FA can be recognized for all OPC replacement levels. In all three graphs, it can be observed that PA performs better than FA and also even better than or similar to 100 % OPC until 20 % GFA. However, at 40 and 60 % GFA, the performance drops down, showing a similar performance to FA. Regardless of that, after 60 % GFA, the performance of FA further declines, while the strength of PA is stabilized, resulting in a higher performance of PA compared to FA. The better 91-day strength performance of PA in all OPC replacement percentages, especially compared to 28-day strength results, indicates a better strength development ability compared to FA. This enhanced strength performance of PA may be attributed to its higher content of alumino-silicate materials (Al_2O_3 and SiO_2) compared to FA, as indicated by the XRF results in Table 1, showing that PA contains 11.2 % more Al_2O_3+SiO_2 than FA. Al_2O_3+SiO_2 react with $Ca(OH)_2$ to form various calcium silicate hydrate (C-S-H) and calcium aluminate hydrate (C-A-H) gels [26], which enhance the strength of the cementitious composite beyond the strength development due to the hydration of cement. This improved pozzolanic activity due to higher Al_2O_3+SiO_2 of PA helps to counter the previously discussed strength-reducing factors that caused the strength reduction in 28-day specimens compared to FA. As the age increases from 28 days to 91 days, the superior pozzolanic ability of PA, attributed to its higher Al_2O_3 + SiO_2 content, results in PA performing better than FA.

5.5. *Strength behaviour of GFA-mortar in relation to ASR*

While it is reasonable to anticipate a negative impact on the strength of GFA-mortar due to the detrimental nature of ASR, the results indicate otherwise. Specifically, no strength reduction was detected in the GFA mortar when aged from 28 to 91 days, even in the 100 % OPC and 100 % GFA mix, which exhibited the highest ASR expansion in the AMBT conditions. At 28 days, the strength of the 100 % GFA mortar showed an 11 % reduction compared to 0 % GFA specimens as shown in Fig. 12. Due to the slow nature of ASR [18, 59], this strength reduction from 0 % to 100 % GFA at 28 days can be attributed to several factors other than ASR, which is discussed in Section 5.3. By 91 days, the strength reduction remained consistent at 10.6 % (Fig. 12). This suggests that ASR has not influenced the strength of the GFA mortar up to at least 91 days, even with 100 % GFA in OPC mortar which showed the highest ASR expansion in AMBT.

Despite the lack of observed strength reduction in GFA-mortar over 91 days, SEM imaging has detected possible early signs of ASR in cube specimens with 100 % GFA, as depicted in Fig. 13(a), since past studies have observed that ASR can occur in the residual cracks of GFA [53]. This indicates that while ASR has not yet adversely affected the strength of the GFA mortar, detrimental effects may emerge as the specimens age further. On the other hand, Figs. 13(b) and 13(c) illustrate the microstructure of 91-day 100 % GFA cube specimens with FA and PA, respectively. Consistent with the discussed ASR mitigation capabilities of both SCMs observed in the AMBT, these specimens show no signs of ASR, highlighting the effectiveness of these pozzolanic SCMs in preventing ASR development in GFA-mortar.

Having observed the trend for the strength development of GFA mortar with OPC from 28 to 91 days, a simple strength testing was carried out for OPC mortar cube specimens with 0 and 100 % GFA subjected to the accelerated ASR conditions (AMBT) for 14 days. The compressive strength of 100 % GFA specimens reported a 23.6 % strength increase compared to the specimen without GFA. Despite the 14-day ASR expansion being high at around 0.2 % with 100 % GFA compared to the 0 % GFA mix, as shown in Fig. 5, the compressive strength is still higher than that of the 0 % GFA mix. If hydration of cement was the only process occurring, the strength of the 100 % GFA mix could not have exceeded that of the 0 % GFA mix, as seen in the normally cured strengths. This is because increased ASR expansion and other factors that reduce strength, as discussed in Section 5.3, should reduce the strength of the 100 % GFA mix compared to the 0 % GFA mix. Therefore, the observed strength increase must be attributed to the reactivity of utilised glass aggregates. Previous studies have documented strength increase due to the pozzolanic activity of glass powder [60–62]. Chen et al. [48] observed this pozzolanic activity even when crushed glass was used as fine aggregate in cementitious mixtures. Furthermore, it has been shown that the pozzolanic reaction of glass particles can be accelerated with an increase in temperature [63]. Thus, the strength increase observed with the 100 % GFA mix is likely due to the pozzolanic activity of the fine glass particles in GFA, which may have been accelerated under AMBT conditions.

6. Conclusions

This study evaluated the properties of GFA-mortar utilizing a widely available reclaimed resource, pond ash as an ASR mitigating SCM. The following conclusions were drawn:

- Up to 60 % of GFA integration is possible when both 28 and 91-day strengths are considered. However, ASR expansion test results reveal that exceeding 20 % GFA incorporation results in detrimental ASR effects, underscoring the necessity of an effective ASR mitigation method.
- At least 20 % of OPC should be replaced with pond ash to effectively mitigate ASR in GFA-mortar, achieving results comparable to fly ash-based ASR mitigation. Similar to fly ash, pond ash reduces the alkalinity of the mix due to its low CaO content, which suppresses ASR. The incorporation of 20 % pond ash enables the use of more than 20 % GFA, potentially up to 100 %.

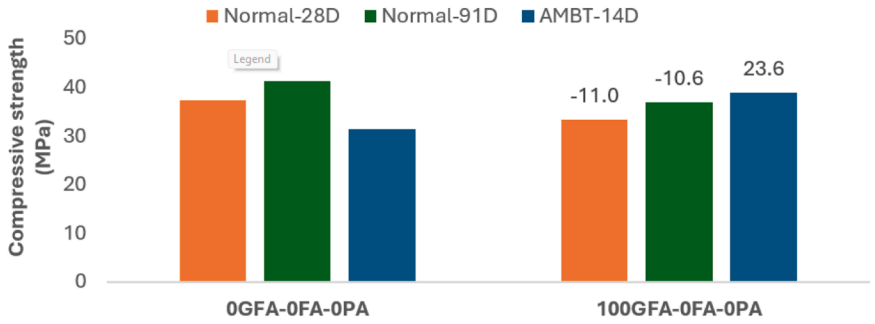

Fig. 12. Compressive strength of mortar cubes cured in normal and AMBT conditions.

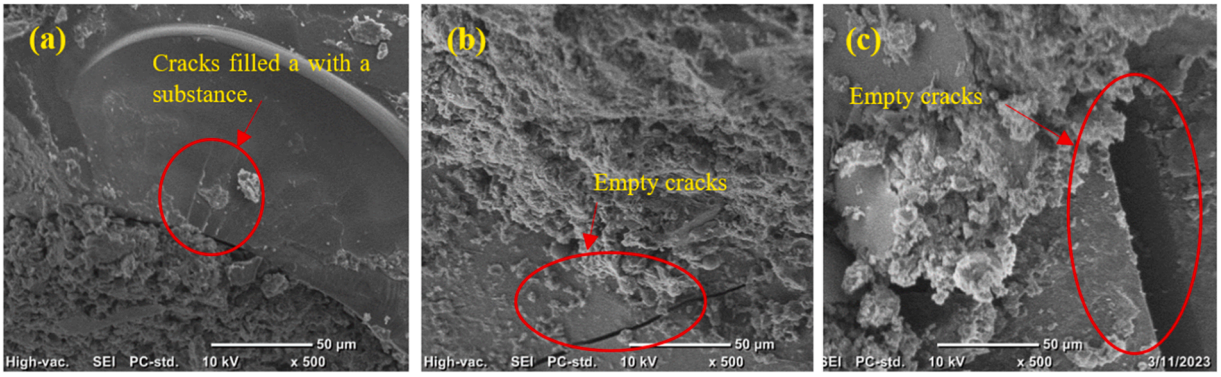

Fig. 13. SEM images of; (a) 100 % GFA and 100 % OPC; (b) 100 % GFA and 30 % FA; (c) 100 % GFA and 30 % PA.

- To achieve strength performance comparable to fly ash at 28 days, only up to 20 % pond ash should be used in GFA-mortar. Higher pond ash content reduces strength due to lower cement hydration and increased flowability, which heightens the risk of segregation in the mix.
- However, at 91 days, pond ash demonstrates superior strength compared to fly ash across nearly all OPC replacement and GFA levels. This is attributed to its enhanced strength development, owing to a higher contents of Al_2O_3 and SiO_2, despite having a larger mean particle size than fly ash.
- For 28-day strength, up to 100 % GFA can be used in combination with 20 % pond ash to achieve performance comparable to fly ash. However, to match the performance of OPC, it is recommended that no more than 20 % GFA be utilised.
- Based on the ASR expansion test and strength results, up to 20 % GFA and 20 % pond ash can be optimally used in mortar, effectively avoiding ASR and significant strength loss. This combination can result in a significantly sustainable mortar.

This study demonstrates that pond ash can be used to partially replace OPC in cementitious mortar with glass fine aggregates, significantly reducing ASR while performing comparably to fly ash in both ASR suppression and strength. However, to utilise pond ash on a larger scale in construction, similar studies should be conducted for concrete and its applications. Additionally, more thorough chemical and microscopical studies are needed to establish the mechanisms by which pond ash affects ASR and the hydration of cement.

Declaration of Competing Interest

The authors declare the following financial interests/personal relationships which may be considered as potential competing interests: Weena Priyanganie Lokuge reports was provided by Australian Research Council (Industrial Transformation Research Hub - research grant IH200100010). Hao Wang reports was provided by Australian Research Council (Industrial Transformation Research Hub - research grant IH200100010). If there are other authors, they declare that they have no known competing financial interests or personal relationships that could have appeared to influence the work reported in this paper.

Acknowledgements

This project is funded by ARC-ITRH (Australian Research Council-Industrial Transformation Research Hub) research grant (IH200100010) allocated for Transformation of Reclaimed Waste Resources to Engineered Materials and Solutions for a Circular

Economy (TREMS). The first author gratefully acknowledged the financial assistance provided by the UniSQ international stipend research scholarship (through TREMS) and the UniSQ international fees research scholarship.

CRediT authorship contribution statement

W.C.V. Fernando: Writing – original draft, Investigation, Formal analysis, Data curation, Conceptualization. **W. Lokuge:** Writing – review & editing, Validation, Supervision, Resources, Project administration, Methodology Funding acquisition, Conceptualization. **H. Wang:** Writing – review & editing, Validation, Supervision, Methodology, Funding acquisition, Conceptualization. **C. Gunasekara:** Writing – review & editing, Validation, Supervision, Methodology, Conceptualization. **K. Dhasindrakrishna**: Writing – review & editing, Investigation, Formal analysis, Data curation.

Data Availability

Data will be made available on request.

References

[1] W. Ferdous, A. Manalo, R. Siddique, P. Mendis, Y. Zhuge, H.S. Wong, W. Lokuge, T. Aravinthan, P. Schubel, Recycling of landfill wastes (tyres, plastics and glass) in construction – a review on global waste generation, performance, application and future opportunities, Resour. Conserv. Recycl. 173 (2021) 105745, https://doi.org/10.1016/J.RESCONREC.2021.105745.
[2] 2021, Nature, Glass is the hidden gem in a carbon-neutral future, 2021. https://doi.org/10.1038/d41586-021-02992-8.
[3] P. Guo, W. Meng, H. Nassif, H. Gou, Y. Bao, New perspectives on recycling waste glass in manufacturing concrete for sustainable civil infrastructure, Constr. Build. Mater. 257 (2020) 119579, https://doi.org/10.1016/J.CONBUILDMAT.2020.119579.
[4] O.M. Olofinnade, J.M. Ndambuki, A.N. Ede, C. Booth, Application of waste glass powder as a partial cement substitute towards more sustainable concrete production, Int. J. Eng. Res. Afr. 31 (2017) 77–93, https://doi.org/10.4028/www.scientific.net/JERA.31.77.
[5] M.M. Disfani, A. Arulrajah, M.W. Bo, N. Sivakugan, Environmental risks of using recycled crushed glass in road applications, J. Clean. Prod. 20 (2012) 170–179, https://doi.org/10.1016/J.JCLEPRO.2011.07.020.
[6] Z.Z. Ismail, E.A. AL-Hashmi, Recycling of waste glass as a partial replacement for fine aggregate in concrete, Waste Manag. 29 (2009) 655–659, https://doi.org/10.1016/j.wasman.2008.08.012.
[7] K. Rashid, R. Hameed, H.A. Ahmad, A. Razzaq, M. Ahmad, A. Mahmood, Analytical framework for value added utilization of glass waste in concrete: mechanical and environmental performance, Waste Manag. 79 (2018) 312–323, https://doi.org/10.1016/j.wasman.2018.07.052.
[8] D.A. Muhedin, R.K. Ibrahim, Effect of waste glass powder as partial replacement of cement & sand in concrete, Case Stud. Constr. Mater. 19 (2023), https://doi.org/10.1016/j.cscm.2023.e02512.
[9] H. Hamada, A. Alattar, B. Tayeh, F. Yahaya, B. Thomas, Effect of recycled waste glass on the properties of high-performance concrete: a critical review, Case Stud. Constr. Mater. 17 (2022), https://doi.org/10.1016/j.cscm.2022.e01149.
[10] C. Polley, S.M. Cramer, R.V. de la Cruz, Potential for using waste glass in Portland cement concrete, J. Mater. Civ. Eng. 10 (1998) 210–219, https://doi.org/10.1061/(asce)0899-1561(1998)10:4(210).
[11] T.M. Borhan, Properties of glass concrete reinforced with short basalt fibre, Mater. Des. 42 (2012) 265–271, https://doi.org/10.1016/j.matdes.2012.05.062.
[12] M. Batayneh, I. Marie, I. Asi, Use of selected waste materials in concrete mixes, Waste Manag. 27 (2007) 1870–1876, https://doi.org/10.1016/j.wasman.2006.07.026.
[13] L.A. Pereira De Oliveira, J.P. Castro-Gomes, P. Santos, Mechanical and durability properties of concrete with ground waste glass sand, 11 DBMC Int. Conf. Durab. Build. Mater. Compon. (2008).
[14] M. Adaway, Y. Wang, Recycled glass as a partial replacement for fine aggregate in structural concrete -effects on compressive strength, Electron. J. Struct. Eng. 14 (2015) 116–122.
[15] N.L. Rahim, R. Che Amat, N.M. Ibrahim, S. Salehuddin, S.A. Mohammed, M. Abdul Rahim, Utilization of recycled glass waste as partial replacement of fine aggregate in concrete production, Mater. Sci. Forum 803 (2015) 16–20, https://doi.org/10.4028/www.scientific.net/MSF.803.16.
[16] S. De Castro, J. De Brito, Evaluation of the durability of concrete made with crushed glass aggregates, J. Clean. Prod. 41 (2013) 7–14, https://doi.org/10.1016/j.jclepro.2012.09.021.
[17] J. Lahdensivu, A. Köliö, D. Husaini, Alkali-silica reaction in Southern-Finland's bridges, Case Stud. Constr. Mater. 8 (2018) 469–475, https://doi.org/10.1016/j.cscm.2018.03.006.
[18] E.O. Fanijo, J.T. Kolawole, A. Almakrab, Alkali-silica reaction (ASR) in concrete structures: mechanisms, effects and evaluation test methods adopted in the United States, Case Stud. Constr. Mater. 15 (2021), https://doi.org/10.1016/j.cscm.2021.e00563.
[19] R.G. Pike, D. Hubbard, Physicochemical studies of the destructive alkali- aggregate reaction in concrete, J. Res Natl. Bur. Stand (1934 59 (1957) 127–132.
[20] C.D. Johnston, Waste glass as coarse aggregate for concrete, J. Test. Eval. 2 (1974) 344–350, https://doi.org/10.1520/JTE10117J.
[21] F. Rajabipour, E. Giannini, C. Dunant, J.H. Ideker, M.D.A. Thomas, Alkali–silica reaction: current understanding of the reaction mechanisms and the knowledge gaps, Cem. Concr. Res 76 (2015) 130–146, https://doi.org/10.1016/j.cemconres.2015.05.024.
[22] S. Abdallah, M. Fan, Characteristics of concrete with waste glass as fine aggregate replacement, Int. J. Eng. Tech. Res. (IJETR 2 (2014) 11–17.
[23] Z. Liu, C. Shi, Q. Shi, X. Tan, W. Meng, Recycling waste glass aggregate in concrete: mitigation of alkali-silica reaction (ASR) by carbonation curing, J. Clean. Prod. 370 (2022) 133545, https://doi.org/10.1016/j.jclepro.2022.133545.
[24] R. Idir, M. Cyr, A. Tagnit-Hamou, Use of fine glass as ASR inhibitor in glass aggregate mortars, Constr. Build. Mater. 24 (2010) 1309–1312, https://doi.org/10.1016/j.conbuildmat.2009.12.030.
[25] J.D. Redondo-Mosquera, D. Sánchez-Angarita, M. Redondo-Pérez, J.C. Gómez-Espitia, J. Abellán-García, Development of high-volume recycled glass ultra-high-performance concrete with high C3A cement, Case Stud. Constr. Mater. 18 (2023), https://doi.org/10.1016/j.cscm.2023.e01906.
[26] S.-Y. Hong, F.P. Glasser, Alkali sorption by C-S-H and C-A-S-H gels: Part II. Role of alumina, Cem. Concr. Res 32 (2002) 1101–1111, https://doi.org/10.1016/S0008-8846(02)00753-6.
[27] S.M.H. Shafaatian, A. Akhavan, H. Maraghechi, F. Rajabipour, How does fly ash mitigate alkali–silica reaction (ASR) in accelerated mortar bar test (ASTM C1567)? Cem. Concr. Compos 37 (2013) 143–153, https://doi.org/10.1016/j.cemconcomp.2012.11.004.
[28] A.S.T.M. International, ASTM C1567 - Standard Test Method for Determining the Potential Alkali-Silica Reactivity of Combinations of Cementitious Materials and Aggregate (Accelerated Mortar-Bar Method), Annu. Book ASTM Stand. (2023).
[29] Y.H. Mugahed Amran, M.G. Soto, R. Alyousef, M. El-Zeadani, H. Alabduljabbar, V. Aune, Performance investigation of high-proportion Saudi-fly-ash-based concrete, Results Eng. 6 (2020) 100118, https://doi.org/10.1016/j.rineng.2020.100118.
[30] M.M. Islam, M.T. Alam, M.S. Islam, Effect of fly ash on freeze–thaw durability of concrete in marine environment, Aust. J. Struct. Eng. 19 (2018) 146–161, https://doi.org/10.1080/13287982.2018.1453332.
[31] A.K. Saha, Effect of class F fly ash on the durability properties of concrete, Sustain. Environ. Res. 28 (2018) 25–31, https://doi.org/10.1016/j.serj.2017.09.001.

[32] R.F. Bleszynski, M.D.A. Thomas, Microstructural studies of alkali-silica reaction in fly ash concrete immersed in alkaline solutions, Adv. Cem. Based Mater. 7 (1998) 66–78, https://doi.org/10.1016/S1065-7355(97)00030-8.
[33] S. Chatterji, A.D. Jensen, N. Thaulow, P. Christensen, Studies of alkali-silica reaction. Part 3. Mechanisms by which NaCl and Ca(OH)2 affect the reaction, Cem. Concr. Res 16 (1986) 246–254, https://doi.org/10.1016/0008-8846(86)90141-9.
[34] Flyash Australia, What is Fly Ash?, (n.d.). https://www.flyashaustralia.com.au/what-is-flyash (accessed December 18, 2024).
[35] F.T.M. Machinery, How to Process Fly Ash and What Is It Used for?, (2023). https://www.ftmmachinery.com/blog/fly-ash-processing-methods-and-equipment.html#toc-heading-1 (accessed December 18, 2024).
[36] Environmental Justice Australia, Unearthing Australia's toxic coal ash legacy, 2019. https://envirojustice.org.au/publication/unearthing-australias-toxic-coal-ash-legacy/ (accessed October 11, 2024).
[37] Y.A. Yimam, G.K. Warati, T. Fantu, V. Paramasivam, S.K. Selvaraj, Effect of pond ash on properties of C-25 concrete, Mater. Today Proc. 46 (2021) 8296–8302, https://doi.org/10.1016/j.matpr.2021.03.258.
[38] D.J. Harris, C. Heidrich, J. Feuerborn, Global aspects on coal combustion products, in: 2019. https://api.semanticscholar.org/CorpusID:254120872.
[39] Ash Development Association of Australia, Annual Production and Utilisation Survey Report, 2023. https://www.adaa.asn.au/resource-utilisation/ccp-utilisation#_ftn1 (accessed October 11, 2024).
[40] B.R. Phanikumar, A. Sofi, Effect of pond ash and steel fibre on engineering properties of concrete, Ain Shams Eng. J. 7 (2016) 89–99, https://doi.org/10.1016/j.asej.2015.03.009.
[41] Y. Patrisia, C. Gunasekara, D.W. Law, T. Loh, K.T.Q. Nguyen, S. Setunge, Optimizing engineering potential in sustainable structural concrete brick utilizing pond ash and unwashed recycled glass sand integration, Case Stud. Constr. Mater. 21 (2024), https://doi.org/10.1016/j.cscm.2024.e03816.
[42] A.S.T.M. International, 2023, ATM C566 - Standard Test Method for Total Evaporable Moisture Content of Aggregate by Drying, Annual Book of ASTM Standards.
[43] ASTM International, ASTM C128 - Standard Test Method for Relative Gravity (Specific Gravity) and Absorption of Fine Aggregate. Annual Book of ASTM Standards, 2022.
[44] ASTM International, ASTM C33/ C33M - Standard Specification for Concrete Aggregates, Annual Book of ASTM Standards (2023).
[45] ASTM International, ASTM C618 - Standard Specification for Coal Ash and Raw or Calcined Natural Pozzolan for Use in Concrete, Annual Book of ASTM Standards, 2023.
[46] ASTM International, ASTM C1437 - Standard Test Method for Flow of Hydraulic Cement Mortar, Annual Book of ASTM Standards, 2020, https://doi.org/10.1520/C1437.
[47] ASTM International, ASTM C109/C109M - Standard Test Method for Compressive Strength of Hydraulic Cement Mortars (Using 2-in. or [50 mm] Cube Specimens), Annual Book of ASTM Standards (2021).
[48] C.H. Chen, R. Huang, J.K. Wu, C.C. Yang, Waste E-glass particles used in cementitious mixtures, Cem. Concr. Res 36 (2006) 449–456, https://doi.org/10.1016/j.cemconres.2005.12.010.
[49] H. Du, K.H. Tan, Effect of particle size on alkali-silica reaction in recycled glass mortars, Constr. Build. Mater. 66 (2014) 275–285, https://doi.org/10.1016/j.conbuildmat.2014.05.092.
[50] F. Rajabipour, H. Maraghechi, G. Fischer, Investigating the Alkali-Silica Reaction of Recycled Glass Aggregates in Concrete Materials, J. Mater. Civ. Eng. 22 (2010) 1201–1208, https://doi.org/10.1061/(asce)mt.1943-5533.0000126.
[51] M.J. Terro, Properties of concrete made with recycled crushed glass at elevated temperatures, Build. Environ. 41 (2006) 633–639, https://doi.org/10.1016/j.buildenv.2005.02.018.
[52] E. Najafi Kani, A.H. Rafiean, A. Alishah, S. Hojjati Astani, S.H. Ghaffar, The effects of Nano-Fe2O3 on the mechanical, physical and microstructure of cementitious composites, Constr. Build. Mater. 266 (2021), https://doi.org/10.1016/j.conbuildmat.2020.121137.
[53] H. Maraghechi, S.M.H. Shafaatian, G. Fischer, F. Rajabipour, The role of residual cracks on alkali silica reactivity of recycled glass aggregates, Cem. Concr. Compos 34 (2012) 41–47, https://doi.org/10.1016/j.cemconcomp.2011.07.004.
[54] N. Damrongwiriyanupap, S. Wongchairattana, T. Phoo-Ngernkham, A. Petcherdchoo, S. Limkatanyu, P. Chindaprasirt, Influence of Recycled Glass on Strength Development of Alkali-Activated High-Calcium Fly Ash Mortar, Adv. Mater. Sci. Eng. (2023), https://doi.org/10.1155/2023/9418619.
[55] T.C. Ling, C.S. Poon, Properties of architectural mortar prepared with recycled glass with different particle sizes, Mater. Des. 32 (2011) 2675–2684, https://doi.org/10.1016/j.matdes.2011.01.011.
[56] F. Moghaddam, V. Sirivivatnanon, K. Vessalas, The effect of fly ash fineness on heat of hydration, microstructure, flow and compressive strength of blended cement pastes, Case Stud. Constr. Mater. 10 (2019), https://doi.org/10.1016/j.cscm.2019.e00218.
[57] R. Kurda, J. de Brito, J.D. Silvestre, Influence of recycled aggregates and high contents of fly ash on concrete fresh properties, Cem. Concr. Compos 84 (2017) 198–213, https://doi.org/10.1016/j.cemconcomp.2017.09.009.
[58] D.K. Nayak, P.P. Abhilash, R. Singh, R. Kumar, V. Kumar, Fly ash for sustainable construction: A review of fly ash concrete and its beneficial use case studies, Clean. Mater. 6 (2022) 100143, https://doi.org/10.1016/j.clema.2022.100143.
[59] A. Saccani, M.C. Bignozzi, ASR expansion behavior of recycled glass fine aggregates in concrete, Cem. Concr. Res 40 (2010) 531–536, https://doi.org/10.1016/j.cemconres.2009.09.003.
[60] K.I.M. Ibrahim, Recycled waste glass powder as a partial replacement of cement in concrete containing silica fume and fly ash, Case Stud. Constr. Mater. 15 (2021), https://doi.org/10.1016/j.cscm.2021.e00630.
[61] K. Afshinnia, P.R. Rangaraju, Influence of fineness of ground recycled glass on mitigation of alkali-silica reaction in mortars, Constr. Build. Mater. 81 (2015) 257–267, https://doi.org/10.1016/j.conbuildmat.2015.02.041.
[62] K. Afshinnia, P.R. Rangaraju, Mitigating alkali-silica reaction in concrete: Effectiveness of ground glass powder from recycled glass, Transp. Res Rec. 2508 (2015) 65–72, https://doi.org/10.3141/2508-08.
[63] M. Mirzahosseini, K.A. Riding, Effect of curing temperature and glass type on the pozzolanic reactivity of glass powder, Cem. Concr. Res 58 (2014) 103–111, https://doi.org/10.1016/j.cemconres.2014.01.015.